https://doi.org/10.1016/j.jsv.2018.01.058 This is the Pre-Published Version.

Optimal design of a beam-based dynamic vibration absorber using fixed-points theory

Yingyu Hua, Waion Wong*, Li Cheng

The Hong Kong Polytechnic University, Department of Mechanical Engineering, Hong Kong SAR, China

Abstract

The addition of a dynamic vibration absorber (DVA) to a vibrating structure could provide an economic solution for vibration suppressions if the absorber is properly designed and located onto the structure. A common design of the DVA is a sprung mass because of its simple structure and low cost. However, the vibration suppression performance of this kind of DVA is limited by the ratio between the absorber mass and the mass of the primary structure . In this paper, a beam-based DVA (beam DVA) is proposed and optimized for minimizing the resonant vibration of a general structure. The vibration suppression performance of the proposed beam DVA depends on the mass ratio, the flexural rigidity and length of the beam. In comparison with the traditional sprung mass DVA, the proposed beam DVA shows more flexibility in vibration control design because it has more design parameters. With proper design, the beam DVA's vibration suppression capability can outperform that of the traditional DVA under the same mass constraint. The general approach is illustrated using a benchmark cantilever beam as an example. The receptance theory is introduced to model the compound system consisting of the host beam and the attached beam-based DVA. The model is validated through comparisons with the results from Abaqus as well as the Transfer Matrix method (TMM) method. Fixed-points theory is then employed to derive the analytical expressions for the optimum tuning ratio and damping ratio of the proposed beam absorber. A design guideline is then presented to choose the parameters of the beam absorber. Comparisons are finally presented between the beam absorber and the traditional DVA in terms of the vibration suppression effect. It is shown that the proposed beam absorber can outperform the traditional DVA by following this proposed guideline.

*Corresponding author. Tel.: +852 27666667

Email address：mmwowong@polyu.edu.hk

1. Introduction

A Dynamic Vibration Absorber (DVA), also known as the tuned mass absorber, is a mechanical device designed to be attached to a primary dynamic structure in order to reduce its vibration or sound radiation. A traditional passive vibration absorber consists of a single degree-of-freedom (SDOF) mass-spring-damper system. The DVA can be used to reduce the unwanted vibration due to a resonant mode or the forced vibration of the primary structure. When properly tuned to deal with the vibration at the targeted frequency, the vibration energy can be transmitted efficiently from the primary structure to the DVA, leading to a reduction in the vibration of the primary structure. DVAs have been extensively applied in civil engineering [1-3] to strengthen the resistance of slender tall buildings subjected to wind loads or seismic excitation.

Many criteria can be found in the literature for the optimal design of tuning frequency and damping ratios of the DVA to maximize its vibration suppression performance [4-7]. The most commonly used one is the H_∞ criterion to minimize the maximum vibration amplitude of the primary structure. Common ways of achieving the H_∞ optimal design of the traditional DVA is to apply the fixed-points theory proposed by Den Hartog in 1928 [4]. The theory states that there exist two fixed points, independent of the damping, in the frequency response spectrum of an undamped SDOF primary system connected with the traditional DVAs. The optimum tuning ratio is determined by making the two fixed points equally high in the spectrum and the optimum damping ratio is determined by making the two fixed points to be the highest points in the response spectrum. The H_∞ design strategy works well for the narrow band control. To tackle the broadband problem like the random excitation, the H_2 optimization criterion can be applied. Warburton [5, 6] derived the optimum tuning ratio and damping ratio in order to minimize the mean square values of the vibration displacement or kinetic energy over a frequency band under various types of external excitations. Asami et al. [7] introduced the damped SDOF primary system and derived the series solution for the H_∞ optimization and the analytical solution for the H_2 optimization of the absorbers parameters. They confirmed that their solution of the optimal absorber parameters could be degenerated to the existing value by Den Hartog's method [4] when the primary system's damping is assumed to be zero.

There are many research works done to extend the fixed-points theory for global vibration control of continuous structures [8][9] and the optimimzation of variant design of DVA [10]. The limitations of the traditional mass spring DVA are mainly in three aspects. a) Their vibration suppression performance is limited once the mass ratio is fixed. Without sufficient absorber mass, the vibration suppression effect is not significant. Due to physical or practical constraints, the absorber mass is seldom larger than 20% of the mass of the primary structure. b) The stiffness of the spring can neither be too high or too low. The spring stiffness can't be too low or else the static displacement will become very large, rendering it difficult to be implemented in practice. If the spring is too hard it can't achieve vibration control at low frequency. c) Their vibration control performance is undermined if the resonance frequency deviates from the targeted value for which they are designed (also known as detuning effect). The solutions to the last question have been attempted by many researchers. The methods include developing active, semi-active or hybrid control devices [11-14] or adaptive vibration absorbers [15] whose stiffness varies with the excitation frequency. These devices are usually bulky and need external energy input. Acar and Yilmaz [16] developed a adaptive absorber consisting of a string-mass system equipped with negative stiffness tension mechanism. Their design allows the absorber's natural frequency to be varied within a certain frequency range by using a small tuning actuator force. This kind of device provides a solution for the bulky and energy-consuming problem in the design of adaptive absorber. However, most of the adaptive absorbers with other physical mechanisms still have the size and energy problems. Meanwhile, strategies involving multiple tuned vibration dampers (MTVD) [17][18] are also investigated to overcome the detuning effect.

As far as the authors know, there is still a lack of effort to address the challenges in a) and b). A beam type DVA which can have better vibration suppression performance under the same mass constraint as compared to the traditional spring mass DVA is proposed. Moreover, this type of DVA can easily control low frequency vibration by using a long beam as the absorber. Aida et al. [19] has reported the optimization of a beam type DVA connected to the host beam through spring and damping element. Under the same boundary constraints, the beam DVA and the host beam can be reduced to a 2-DOF system, and then the fixed-points theory is used to obtain the optimum tuning ratio and damping ratio. In their optimization method, the vibration control effect of the beam type DVA is still dependent on the mass ratio between the two beams. Moreover, the spring and damping element are required to be accurately manufactured to their optimum value. On the other hand, the proposed beam DVA of this paper doesn't require any extra stiffness element and its vibration control effect is not solely

dependent on the mass ratio. The working principle of the proposed beam DVA is described in Sections 3 and 6 of this paper.

The idea of the beam-based dynamic vibration absorber proposed in this paper was inspired by the work of Tso et al. [14] as shown in Fig. 1, in which a hybrid DVA capable of achieving the global control in a broadband vibration of a primary beam structure is established. This hybrid DVA has a passive control part consisting of a rotational beam structure with a lumped mass. Similarly, the passive dynamic vibration absorber used in this paper consists of a rotational beam structure with viscous damping which is optimized based on the fixed-points theory. This basic configuration lays the foundation for developing more complicated absorbers based on the continuous beam structure, by attaching a lumped mass at the free end of the beam, adding constrained damping layer to the beam, etc.

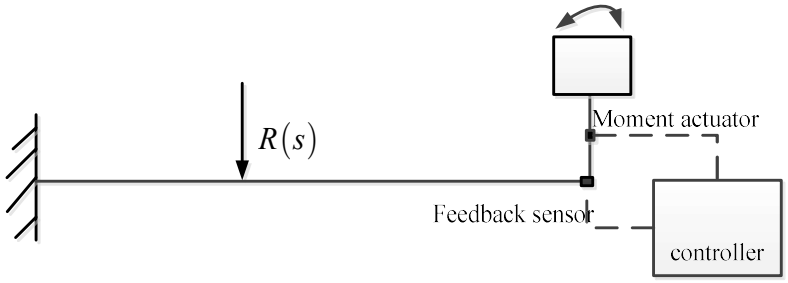

Fig.1. A cantilever beam carrying the proposed HVA at the end of the beam [14]

The layout of this paper is arranged as follows. In Section 2, the receptance theory is introduced to derive the receptance expression of a general structure attached with a general DVA. To illustrate the verification of the receptance theory, the detailed modeling of the L-shaped compound system is presented in Section 3. The receptance of beam absorber, is defined as the ratio of the rotational angle from the attached point to the moment transferred to the primary beam. The continuous conditions at the connecting point include the equivalence of the rotation angle, shear force and moment at the connecting point. The receptance expression of the cantilever primary beam according to similar procedure in Section 2 can be derived. In Section 4, a specific case study is used to validate the modeling method by comparing the results with these from Abaqus and Transfer Matrix Method(TMM). In Section 5, the fixed points are shown to exist, which are independent of the damping ratio in the beam absorber. The fixed-points theory is then used to obtain the analytical formula of the optimum tuning ratio and damping ratio. In Section 6, the relationship of the tuning ratio with the physical parameters of the compound system is demonstrated. A guideline for designing the beam absorber is then given. In Section 7, a comparison of the beam absorber

and the traditional DVA in vibration suppression performance is conducted. It is shown that the beam absorber can outperform the traditional DVA when the geometry is properly designed. Conclusions are presented with future work being discussed in Section 8.

2. Receptance theory of a general dynamic structure connected with a discrete DVA

In this Section, a brief review of the receptance theory is presented first and then the receptance theory is applied to obtain the displacement response of a multimode system connected with a traditional DVA (i.e., mass-spring-damper) under external harmonic force excitation.

2.1 Modal receptance of a dynamic structure

When a system is subjected to a general harmonic unit excitation, its vibration response is called the receptance [20]. The so-called response can be defined as the complex harmonic displacement or rotation due to a unit real harmonic force or moment.

Consider a multimode system subjected to a single harmonic force $F\cos\omega t$ at (x_s, y_s) as shown in Fig. 2(a).

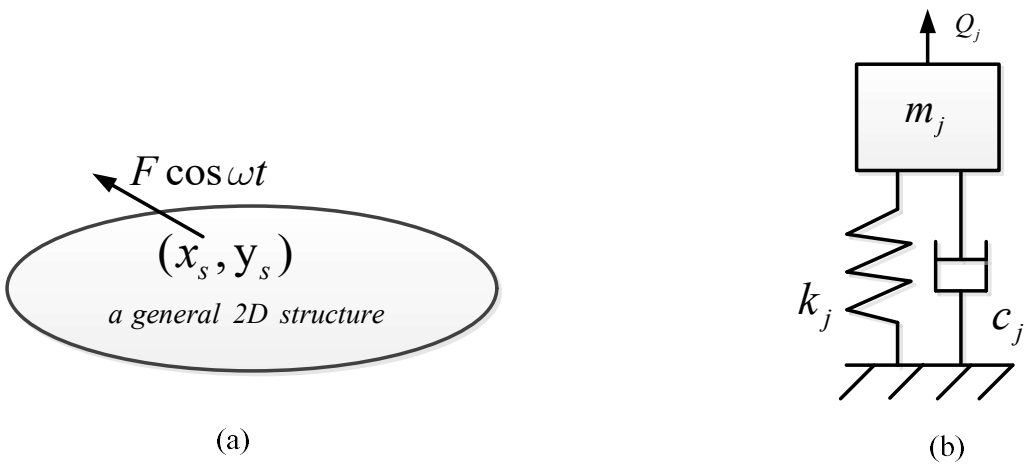

Fig. 2 (a) The general structure subjected to a harmonic external concentrated force

(b) The mass-spring-damper system in the j^{th} mode coordinate

The generalized equation of motion in the j^{th} modal coordinate as shown in Fig. 2(b) is given by

$$m_j\ddot{q}_j + c_j\dot{q}_j + k_j q_j = Q_j = \mathrm{Re}\left[F\phi_j(x_s, y_s)e^{i\omega t}\right] \tag{1}$$

where m_j, c_j, k_j are the modal mass, damping loss coefficient, and stiffness, respectively, corresponding to the j^{th} mode of the dynamic system. The right-hand side of Eq. (1) represents the real part of the complex dynamic response. $\phi_j(x, y)$ is the j^{th} mode shape function. $F\phi_j(x_s, y_s)$ is the magnitude of the general force Q_j exerting on the j^{th} mode. The receptance of the j^{th} mode represents the complex displacement due to a unit real force in the decoupled j^{th} mode system written as

$$\alpha_{jj} = \frac{1}{m_j(\Omega_j^2 - \omega^2 + i2\xi_j\Omega_j\omega)} \tag{2}$$

where $\Omega_j = \sqrt{k_j/m_j}, \xi_j = c_j/2\sqrt{k_j m_j}$ are the j^{th} modal frequency and damping loss factor respectively.

Thus, the displacement at any point (x, y) writes

$$\begin{aligned} w(x,y,t) &= \mathrm{Re}\left[\sum_{j=1}^{\infty}\frac{F\phi_j(x,y)\phi_j(x_s,y_s)e^{i\omega t}}{-m_j\omega^2 + c_j\omega i + k_j}\right] = \mathrm{Re}\left[\sum_{j=1}^{\infty}\frac{F\phi_j(x,y)\phi_j(x_s,y_s)e^{i\omega t}}{m_j(\Omega_j^2 - \omega^2 + 2\xi_j\Omega_j\omega i)}\right] \\ &= \mathrm{Re}\left[\sum_{j=1}^{\infty}\frac{F\phi_j(x,y)\phi_j(x_s,y_s)e^{i\omega t}}{k_j(\Omega_j^2 - \omega^2 + 2\xi_j\Omega_j\omega i)}\right] = \mathrm{Re}\left[\sum_{j=1}^{\infty}F\phi_j(x,y)\alpha_{jj}\phi_j(x_s,y_s)e^{i\omega t}\right] \end{aligned} \tag{3}$$

2.2 The receptance of a dynamic structure connected with a DVA under external force

Consider the case when a traditional DVA is connected to the primary structure at (x_s, y_s) with a harmonic external force $\mathrm{Re}(F_e e(i\omega t))$ exerted at (x_e, y_e) of the structure as shown in Fig. 3.

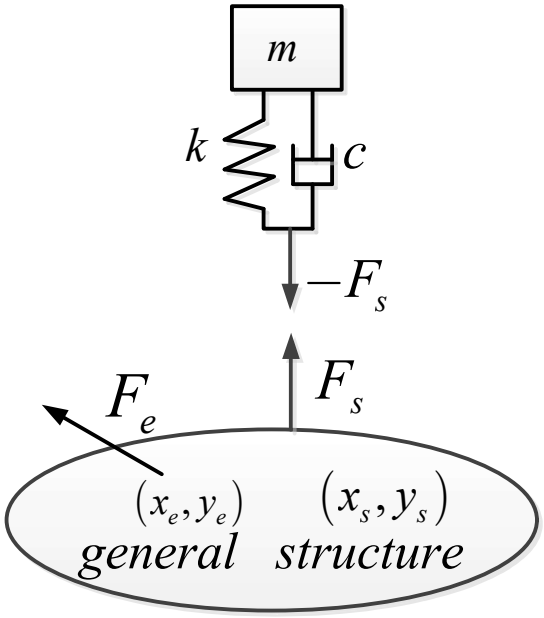

Fig 3. A dynamic structure connected with a mass-spring- damper

The reaction force of the DVA on the primary structure is $-\mathrm{Re}(F_s \exp i\omega t)$. Let α_{aux} and $W(x_s, y_s)$ represent the receptance of the DVA and the complex displacement at the connecting point (x_s, y_s), respectively. The displacement $W(x_s, y_s)$ can be related to the magnitude of the reacting force F_s as

$$W(x_s, y_s) = -\alpha_{aux} F_s \tag{4}$$

According to Eq. (2), the displacement of the primary structure at point (x, y) due to the reaction force of DVA, $\mathrm{Re}(F_s e^{i\omega t})$, and the external force $\mathrm{Re}(F_e e^{i\omega t})$ can be written as

$$W(x, y) = \sum_{j=1}^{\infty} \phi_j(x, y)\alpha_{jj}\phi_j(x_s, y_s)F_s + \sum_{j=1}^{\infty} \phi_j(x, y)\alpha_{jj}\phi_j(x_e, y_e)F_e \tag{5}$$

The complex displacement of the primary structure at the connecting point (x_s, y_s) is therefore written as

$$W(x_s, y_s) = \sum_{j=1}^{\infty} \phi_j(x_s, y_s)\alpha_{jj}\phi_j(x_s, y_s)F_s + \sum_{j=1}^{\infty} \phi_j(x_s, y_s)\alpha_{jj}\phi_j(x_e, y_e)F_e \tag{6}$$

Substituting Eq. (4) to Eq. (6) gives the complex displacement at point (x_s, y_s) written as

$$W(x_s,y_s)=\sum_{j=1}^{\infty}\phi_j(x_s,y_s)\alpha_{jj}\phi_j(x_s,y_s)\left(-\frac{W(x_s,y_s)}{\alpha_{aux}}\right)+\sum_{j=1}^{\infty}\phi_j(x_s,y_s)\alpha_{jj}\phi_j(x_e,y_e)F_e$$

$$=\frac{\sum_{j=1}^{\infty}\phi_j(x_s,y_s)\phi_j(x_e,y_e)\alpha_{jj}}{1+\sum_{j=1}^{\infty}\left[\phi_j(x_s,y_s)\right]^2\frac{\alpha_{jj}}{\alpha_{aux}}}F_e \tag{7}$$

Substituting Eq. (7) to Eq. (6) gives the complex displacement at point (x,y) written as

$$\frac{W(x,y)}{F_e}=\left\{\sum_{j=1}^{\infty}\phi_j(x,y)\alpha_{jj}\phi_j(x_s,y_s)\left[-\frac{W(x_s,y_s)}{\alpha_{aux}}\right]+\sum_{j=1}^{\infty}\phi_j(x,y)\alpha_{jj}\phi_j(x_e,y_e)F_e\right\}\Big/F_e$$

$$=\sum_{j=1}^{\infty}\phi_j(x,y)\alpha_{jj}\left[-\phi_j(x_s,y_s)\frac{\sum_{k=1}^{\infty}\phi_k(x_s,y_s)\phi_k(x_e,y_e)\frac{\alpha_{kk}}{\alpha_{aux}}}{1+\sum_{j=1}^{\infty}\left[\phi_k(x_s,y_s)\right]^2\frac{\alpha_{kk}}{\alpha_{aux}}}+\phi_j(x_e,y_e)\right]F_e/F_e$$

$$=\frac{\sum_{j=1}^{\infty}\left\{\phi_j(x,y)\phi_j(x_e,y_e)\alpha_{jj}-\phi_j(x,y)\alpha_{jj}\phi_j(x_s,y_s)\sum_{k=1}^{\infty}\phi_k(x_s,y_s)\phi_k(x_e,y_e)\frac{\alpha_{kk}}{\alpha_{aux}}+\phi_j(x,y)\alpha_{jj}\phi_j(x_e,y_e)\sum_{k=1}^{\infty}\left[\phi_k(x_s,y_s)\right]^2\frac{\alpha_{kk}}{\alpha_{aux}}\right\}}{1+\sum_{k=1}^{\infty}\left[\phi_k(x_s,y_s)\right]^2\frac{\alpha_{kk}}{\alpha_{aux}}} \tag{8}$$

From Eq. (8), it can be seen that the receptance of the primary structure connected with a DVA depends on both the modal characters of the primary structure and the receptance α_{aux} of the DVA. It should also be noted that although the DVA is depicted as the traditional SDOF mass-spring-damper design in Fig.3, its design can be generalized to include the proposed continuous beam absorber as well. Hence, in the beam absorber case, the reaction force from the DVA is the turning moment. The receptance of Eq. (4) should become the rotational angle of the connecting point divided by the reactional moment from the DVA to the primary structure.

3. Analytical model of the L-shape beam system

Consider a L-shape beam system as shown in Fig. 4. The primary beam is excited by the distributed force $r(t)$ covering area $g(x_1)$ of the beam. In the following analysis, subscripts 1 and 2 stand for the primary beam and the beam absorber, respectively.

Coordinates x_1 and x_2 are along the axial directions of the primary beam and the beam absorber, respectively.

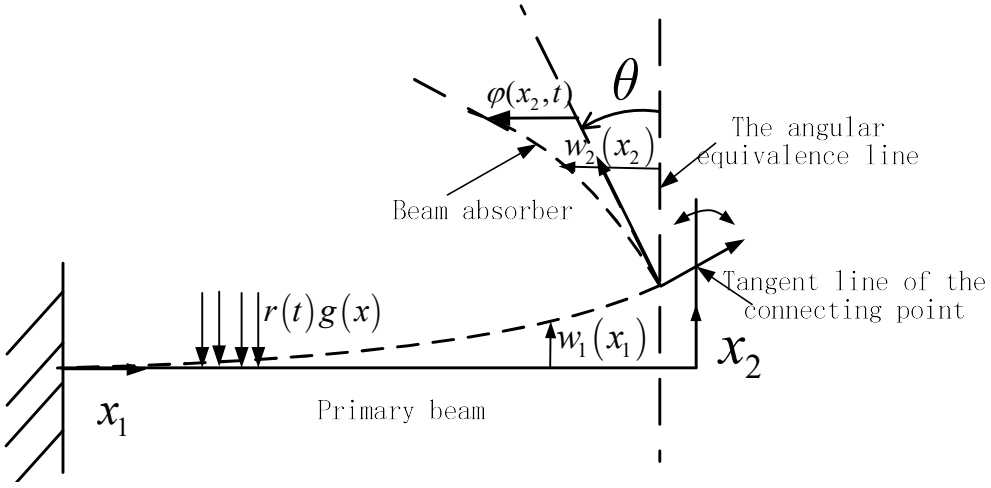

Fig.4. The model of L shaped beam system

The equation of motion of the primary beam is written as

$$\rho_1 A_1 \ddot{w}_1 + E_1 I_1 w_1'''' = r(t)g(x_1) \tag{9}$$

Based on the damping mechanism of the beam [21], the beam with viscous damping is used to model the beam absorber as:

$$E_2 I_2 \frac{\partial^4 \varphi(x_2,t)}{\partial x_2^4} + c\frac{\partial \varphi(x_2,t)}{\partial t} + \rho_2 A_2 \frac{\partial^2 \varphi(x_2,t)}{\partial t^2} = -c\dot{\theta}(t)x_2 - \rho_2 A_2 \ddot{\theta}(t)x_2 \tag{10}$$

The general flexural displacement of the beam absorber is

$$w_2(x_2,t) = \theta(t)x_2 + \varphi(x_2,t) \tag{11}$$

where $\theta(t)$ is the rotational angle from the connecting point transmitted to the beam absorber and $\varphi(x_2,t)$ is the deflection due to strain deformation in the beam absorber. The beam absorber is modeled as a cantilever beam subjected to the rotational motion from the clamped end. The detailed modeling of the beam absorber is given in Appendix A.

The continuous conditions at the connecting point between the primary structure and the beam absorber may be written as in [22]:

$$\begin{cases} w_2(0,t)=0 \\ w_2'(0,t)=w_1'(L_1,t)=\theta(t) \\ E_1I_1w_1'''(L_1,t)=m_2\ddot{w}_1(L_1,t) \\ E_1I_1w_1''(L_1,t)=M\left(t\right) \end{cases} \tag{12}$$

where m_2 is the mass of the beam absorber and $M\left(t\right)$ is the reaction moment exerted by the beam absorber on the primary beam.

The mode shape functions of the primary cantilever beam structure satisfy the mass orthogonality and normalization principle. They can be written as

$$\begin{aligned} &\phi_{1i}(x_1)=A_{1i}\left\{\cos(b_ix_1/L_1)-\cosh(b_ix_1/L_1)+r_{1i}\left[\sin(b_ix_1/L_1)-\sinh(b_ix_1/L_1)\right]\right\} \\ &r_{1i}=-\left[\cos(b_i)+\cosh(b_i)\right]/\left[\sin(b_i)+\sinh(b_i)\right] \end{aligned} \tag{13}$$

$$\begin{aligned} &\int_0^{L_1}\rho_1A_1\phi_{1i}(x_1)\phi_{1j}(x_1)dx_1=\delta_{ij}=\begin{cases}1, i=j \\ 0, i\neq j\end{cases} \qquad i,j=1,2,3\cdots \\ &E_1I_1\int_0^{L_1}\phi_{1i}''(x_1)\phi_{1j}''(x_1)dx_1=\Omega_i^2\delta_{ij} \end{aligned} \tag{14}$$

where $\cos b_i\cosh b_i=-1$, and b_i takes the values of 1.875, 4.694 and 7.855 for the first three modes of a cantilever beam. Using Eqs. (9), (12) and (14), the response of the primary structure can be projected to the modal coordinate:

$$\begin{aligned} &E_1I_1w_1'''(x_1,t)\phi_{1j}(x_1)\Big|_0^{L_1}-E_1I_1w_1''(x_1,t)\phi_{1j}'(x_1)\Big|_0^{L_1}+\sum_{i=1}^{\infty}\int_0^{L_1}E_1I_1\phi_{1i}''(x_1)\phi_{1j}''(x_1)dx_1q_{1i}(t) \\ &+\sum_{i=1}^{\infty}\int_0^{L_1}\rho_1A_1\phi_{1i}(x_1)\phi_{1j}(x_1)dx_1\ddot{q}_{1i}(t)=r(t)\int_0^{L_1}g(x_1)\phi_{1j}(x_1)dx_1 \end{aligned} \tag{15}$$

Using the boundary conditions in Eq. (12), Eq. (15) can be written as

$$\begin{aligned} &\sum_{i=1}^{\infty}\int_0^{L_1}E_1I_1\phi_{1i}''(x_1)\phi_{1j}''(x_1)dx_1q_{1i}(t)+\sum_{i=1}^{\infty}\int_0^{L_1}\rho_1A_1\phi_{1i}(x_1)\phi_{1j}(x_1)dx_1\ddot{q}_{1i}(t) \\ &+m_2\sum_{i=1}^{\infty}\phi_{1i}(L_1)\phi_{1j}(L_1)\ddot{q}_{1i}(t)=M\left(t\right)\phi_{1j}'(L_1)+r(t)\int_0^{L_1}g(x_1)\phi_{1j}(x_1)dx_1 \end{aligned} \tag{16}$$

Applying Laplace transformation to Eq. (16) and making use of the orthogonality and the normalization conditions in Eq. (14), Eq. (16) may be written as

$$\begin{aligned} &\left[\Omega_i^2+(1+\mu_i)s^2\right]Q_{1i}(\mathrm{s})=\tilde{M}\left(s\right)\phi_{1i}'(L_1)+R(s)\int_0^{L_1}g(x_1)\phi_{1i}(x_1)dx_1 \\ &\mu_i=m_2\phi_{1i}^2(L_1) \end{aligned} \tag{17}$$

where $\tilde{M}(s) = Laplace(M(t))$ (18)

The angular displacement of the DVA can be related to the reaction moment and written as

$$\tilde{\theta}(s) = \alpha_{aux}\tilde{M}(s) \tag{19}$$

where $\tilde{\theta}(s) = Laplace(\theta(t))$ (20)

Substituting Eq.(19) to Eq.(17), the flexural displacement of the primary beam can be written as

$$\begin{aligned} W_1(x_1,\mathrm{s}) &= \sum_{j=1}^{\infty}\phi_{1j}(x_1)\alpha_{jj}\phi'_{1j}(L_1)\tilde{M} + \sum_{j=1}^{\infty}\phi_{1j}(x_1)\alpha_{jj}R(s)\int_0^{L_1} g(x_1)\phi_{1j}(x_1)dx_1 \\ &= \sum_{j=1}^{\infty}\phi_{1j}(x_1)\alpha_{jj}\phi'_{1j}(L_1)\frac{\tilde{\theta}(s)}{\alpha_{aux}} + \sum_{j=1}^{\infty}\phi_{1j}(x_1)\alpha_{jj}R(s)\int_0^{L_1} g(x_1)\phi_{1j}(x_1)dx_1 \end{aligned} \tag{21}$$

where $\alpha_{jj} = 1\Big/\left[\Omega_j^2 + (1+\mu_j)s^2\right]$ (22)

The rotational angle at the attached point of the beam absorber can be written as

$$\begin{aligned} \tilde{\theta}(s) &= -W_1'(L_1,\mathrm{s}) \\ &= -\sum_{j=1}^{\infty}\phi'_{1j}(L_1)\alpha_{jj}\phi'_{1j}(L_1)\frac{\tilde{\theta}(s)}{\alpha_{aux}} - \sum_{j=1}^{\infty}\phi'_{1j}(L_1)\alpha_{jj}R(s)\int_0^{L_1} g(x_1)\phi_{1j}(x_1)dx_1 \\ &= -\frac{\sum_{j=1}^{\infty}\phi'_{1j}(L_1)\alpha_{jj}\int_0^{L_1} g(x_1)\phi_{1j}(x_1)dx_1}{1+\sum_{j=1}^{\infty}\phi'_{1j}(L_1)^2\frac{\alpha_{jj}}{\alpha_{aux}}}R(s) \end{aligned} \tag{23}$$

Substituting Eq. (23) to Eq. (21) gives

$$\frac{W_1(x_1,\mathrm{s})}{\tilde{R}(s)} = \frac{-\sum_{i=1}^{\infty}\left[\frac{\phi_{1i}(x_1)\alpha_{ii}\phi'_{1i}(L_1)}{\alpha_{aux}}\sum_{j=1}^{\infty}\alpha_{jj}\phi'_{1j}(L_1) - \alpha_{ii}\phi_{1i}(x_1)\sum_{j=1}^{\infty}\frac{\alpha_{jj}\phi'_{1j}(L_1)^2}{\alpha_{aux}} - \phi_{1i}(x_1)\alpha_{ii}\right]\int_0^{L_1} g(x_1)\phi_{1i}(x_1)dx_1}{1+\sum_{j=1}^{\infty}\phi'_{1j}(L_1)^2\frac{\alpha_{jj}}{\alpha_{aux}}} \tag{24}$$

The term α_{aux} depends on the specific physical configuration of the beam absorber. Using modal decomposition in Eq. (10) yields:

$$\omega_i^2 q_{2i}(t) + 2\xi_i\omega_i\dot{q}_{2i}(t) + \ddot{q}_{2i}(t) = -\rho_2 A_2\int_0^{L_2} x_2\phi_{2i}(x_2)dx_2(\ddot{\theta}(t) + 2\xi_i\omega_i\dot{\theta}(t)) \tag{25}$$

where $\phi_{2i}(x_2)$ is the *ith* mode shape of the cantilever beam and satisfies the mass orthogonality and normalization condition as follows

$$\phi_{2i}(x_2) = A_{2i}\left\{\cos(b_i x_2 / L_2) - \cosh(b_i x_2 / L_2) + r_{2i}\left[\sin(b_i x_2 / L_2) - \sinh(b_i x_2 / L_2)\right]\right\} \quad (26)$$
$$r_{2i} = -\left[\cos(b_i) + \cosh(b_i)\right] / \left[\sin(b_i) + \sinh(b_i)\right]$$

$$\int_0^{L_2} \rho_2 A_2 \phi_{2i}(x_2)\phi_{2j}(x_2)dx_2 = \delta_{ij} = \begin{cases} 1, i = j \\ 0, i \neq j \end{cases} \qquad i, j = 1, 2, 3\cdots \quad (27)$$
$$E_2 I_2 \int_0^{L_2} \phi_{2i}''(x_2)\phi_{2j}''(x_2)dx_2 = \omega_i^2 \delta_{ij}$$

The modal damping ratio ξ_i is defined as

$$\xi_i = c/\left(2\rho_2 A_2 \omega_i\right) \quad (28)$$

Applying Laplace transformation to Eq. (11), we may write

$$W_2(x_2, s) = \tilde{\theta}(\mathrm{s})x_2 + \Psi\left(x_2, s\right) \quad (29)$$
$$W_2(x_2, s) = Laplace(w_2(x_2, t)), \Psi\left(x_2, s\right) = Laplace\left(\varphi(x_2, t)\right)$$

Applying Laplace transformation to Eq. (25), we may write

$$\Psi\left(x_2, s\right) = \sum_{i=1}^{\infty} \phi_{2i}\left(x_2\right) \frac{g_i\left(s^2 + 2\xi_i\omega_i s\right)}{s^2 + 2\xi_i\omega_i s + \omega_i^2} \tilde{\theta}\left(s\right) \quad (30)$$

where $g_i = -\rho_2 A_2 \int_0^{L_2} x_2 \phi_{2i}(x_2)dx_2$ (31)

The receptance of the beam absorber can be written as

$$1/\alpha_{\text{aux}} = \tilde{M}/\tilde{\theta} = -E_2 I_2 W_2''(0, s)/\tilde{\theta} = -E_2 I_2 \Psi''(0, s)/\tilde{\theta}$$
$$= \sum_{i=1}^{\infty} -E_2 I_2 \phi_{2i}''(0) \frac{g_i\left(s^2 + 2\xi_i\omega_i s\right)}{s^2 + 2\xi_i\omega_i s + \omega_i^2} \quad (32)$$

4. Validation of the modeling method

A numerical case is presented in the following to validate the accuracy of the proposed modeling method by comparing the results with the finite element analysis using Abaqus and the TMM method. The material and geometric properties of the primary beam and beam absorber are listed in Table 1.

Table 1. The material property and geometry size of the primary and beam absorber

	Density/ kg/m^3	Young's modulus/ Gpa	Length/ mm	Width/ mm	Thickness/ mm
Primary beam	7890	206	515.75	12.7	4
Beam absorber	2766	69	177.8	12.7	3.05

In this validation study, both the primary and absorber beam dampings are set to zero. So $\xi_i = 0$ in Eq. (32). The primary structure is subjected to a white noise signal at the middle of the span. So $g(x) = \delta(x - 0.5L_1)$ in Eq. (24). Consider the first three modes of the cantilever beam according to Eq. (24), the receptance at the end of the beam can be written as:

$$\frac{W_1(L_1,s)}{R(s)} = \frac{-\sum_{i=1}^{3}\left[\frac{\phi_{1i}(L_1)\alpha_{ii}\phi'_{1i}(L_1)}{\alpha_{aux}}\sum_{j=1}^{3}\alpha_{jj}\phi'_{1j}(L_1) - \alpha_{ii}\phi_{1i}(L_1)\sum_{j=1}^{3}\frac{\alpha_{jj}\phi'_{1j}(L_1)^2}{\alpha_{aux}} - \phi_{1i}(L_1)\alpha_{ii}\right]}{1+\sum_{j=1}^{3}\phi'_{1j}(L_1)^2\frac{\alpha_{jj}}{\alpha_{aux}}}\phi_{1i}(0.5L_1) \tag{33}$$

where $1/\alpha_{aux}$ is the summation of the first fifty terms in Eq.(32) and α_{jj} is calculated according to Eq. (22).

The receptance at the end of the primary beam is calculated by three different methods: Abaqus, TMM and the receptance theory in Section 3 and the numerical results are plotted in Fig. 5 for comparison. The receptance theory uses the first three modes in the primary beam and the first fifty modes of the beam absorber as shown in Eq. (33). In Abaqus analysis, B21 element is used to model the L-shaped beam system. The direct steady state analysis is conducted to get the displacement response at the end of the primary beam. The TMM method comes from the dynamic stiffness matrix method, which is briefly introduced in Appendix B.

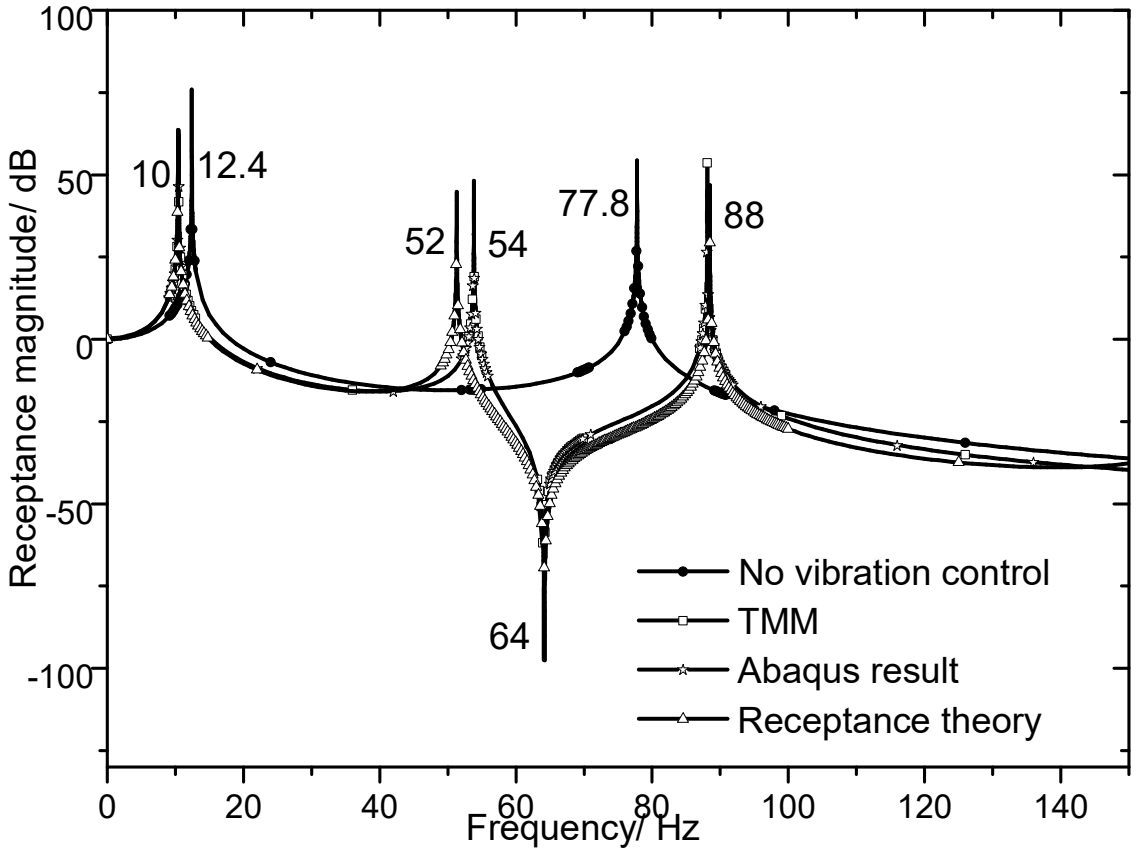

Fig. 5. Receptance magnitude $\left|W_1(L_1,s)/R(s)\right|$ at the end of the primary beam with and without absorber

In this case, the first two natural frequencies of the primary beam are 12.4 Hz and 77.8 Hz. The first natural frequency of the beam absorber is 77.8 Hz. Fig. 5 shows the typical phenomenon with the fundamental DVA theory that the original second order resonance is suppressed at the cost of two newly appearing peaks.

In Fig.5, the frequency responses by the three methods match very well at the resonant frequencies of the first and third vibration modes and also at the antiresonant frequency. The resonant frequency of the second mode is found to be 52Hz using the receptance theory, and 54Hz by both the Abaqus and TMM methods. This difference may be due to the ignorance of the axial deformation and the coupling between the axial and flexural movements in the host beam and beam DVA when using the receptance theory. On the other hand, the TMM method and Abaqus both take the axial deformation and the coupling between axial and flexural movement into account. In conclusion, besides the small difference, the receptance theory can still be used to predict a good approximation of the frequency response of the compound beam system.

5. The optimum parameters of the fixed-points theory

When the N^{th} order resonance frequency of the primary beam is close to the r^{th} order resonance frequency of the beam absorber, Eq. (24) can be simplified to describe the contribution from the N^{th} order mode of the primary beam and α_{aux} to that from the r^{th} order mode of the beam absorber. For the sake of convenience, all the receptance terms in Eqs. (22), (24) and (32) are transformed to the dimensionless form.

$$\alpha_{NN} = 1/\left[\Omega_N^2 - (1+\mu_N)\omega^2\right] = 1/\Omega_N^2\left[1-f^2\right] \tag{34}$$

$$\begin{aligned} 1/\alpha_{\text{aux}} &= \tilde{M}/\tilde{\theta} \\ &= -E_2 I_2 \phi_{2r}''(0)\frac{g_r\left(-\omega^2 + 2\xi_r\omega_r\omega i\right)}{-\omega^2 + 2\xi_i\omega_i\omega i + \omega_i^2} \\ &= -E_2 I_2 \phi_{2r}''(0) g_r \frac{\left(-f^2 + i2\xi_r\lambda f\right)}{-f^2 + i2\xi_r\lambda f + \lambda^2} \end{aligned} \tag{35}$$

$$\begin{aligned} H(x_1,s) &= \frac{W_1(x_1,s)}{R(s)\int_0^{L_1} g(x_1)\phi_{1N}(x_1)dx_1} = \frac{\phi_{1N}(x_1)\alpha_{NN}}{1+\phi_{1N}'(L_1)^2\dfrac{\alpha_{NN}}{\alpha_{aux}}} \\ &= \frac{\phi_{1N}(x_1)}{\Omega_N^2}\frac{\left(\lambda^2 - f^2 + i2\xi_r\lambda f\right)}{\left[\left(1-f^2\right)\left(\lambda^2-f^2\right) - \varepsilon f^2\right] + i2\xi_r\lambda f\left(1+\varepsilon-f^2\right)} \end{aligned} \tag{36}$$

where

$$\bar{\Omega}_N^2 = \Omega_N^2/(1+\mu_N),\ f = \omega/\bar{\Omega}_N,\ \lambda = \omega_r/\bar{\Omega}_N \tag{37}$$

$$\begin{aligned} \varepsilon &= -E_2 I_2 \phi_{2r}''(0) g_r \phi_{1N}'(L_1)^2/\Omega_N^2 \\ &= E_2 I_2 \phi_{2r}''(0)\phi_{1N}'(L_1)^2 \rho_2 A_2 \int_0^{L_2} x_2\phi_{2r}(x_2)dx_2 \Big/ \Omega_N^2 \end{aligned} \tag{38}$$

The dimensionless form of the receptance in Eq. (36) can be written as

$$\tilde{H}(f) = \frac{\left(\lambda^2 - f^2 + i2\xi_r\lambda f\right)}{\left[\left(1-f^2\right)\left(\lambda^2-f^2\right) - \varepsilon f^2\right] + i2\xi_r\lambda f\left(1+\varepsilon-f^2\right)} \tag{39}$$

To study the effect of the damping ξ_r on the receptance $\tilde{H}(f)$, three values of ξ_r (0, 0.3 and ∞) with ε, λ and μ_N calculated from Table 1 are used to calculate $\tilde{H}(f)$ using Eq. (39) and its magnitude $\left|\tilde{H}(f)\right|$ is plotted in Fig. 6. It can be observed from Fig. 6 that the

dimensionless magnitude $\left|\tilde{H}(f)\right|$ has two fixed points which are independent of the damping ratio. It shows that the fixed-points theory can be employed to obtain the optimum tuning ratio and damping ratio of the proposed DVA.

$$\frac{\lambda^2 - f^2}{\left(1-f^2\right)\left(\lambda^2 - f^2\right) - \varepsilon f^2} = \pm\frac{1}{1+\varepsilon-f^2}$$
$$\left|\tilde{H}(f_1)\right| = \left|\tilde{H}(f_2)\right| \tag{40}$$

$$\lambda_{opt} = \sqrt{1+\varepsilon},$$
$$f_{1,2}^2 = \varepsilon + 1 \pm \sqrt{\left(\varepsilon^2+\varepsilon\right)/2} \tag{41}$$
$$\left|\tilde{H}(f_1)\right|^2 = \left|\tilde{H}(f_2)\right|^2 = 2/\left(\varepsilon^2+\varepsilon\right)$$

Thus the magnitudes of the two fixed points are made equal.

$$\left|\tilde{H}_b(f)\right|^2 = \frac{\left(\lambda^2-f^2\right)^2 + \left(2\xi_r\lambda f\right)^2}{\left[\left(1-f^2\right)\left(\lambda^2-f^2\right) - \varepsilon f^2\right]^2 + \left[2\xi_r\lambda f\left(1+\varepsilon-f^2\right)\right]^2} = \frac{p}{q}$$
$$\left.\frac{\partial\left|\tilde{H}_b(f)\right|^2}{\partial f^2}\right|_{f_1,f_2} = 0 \Leftrightarrow \frac{\partial p}{\partial f^2} - \frac{p}{q}\frac{\partial q}{\partial f^2}\Big|_{f=f_1,f_2} = 0 \tag{42}$$

$$\xi_r^2\Big|_{f_1} = \frac{3}{4}\frac{u}{(\varepsilon+1)^2 - (\varepsilon+1)\sqrt{u}}$$
$$\xi_r^2\Big|_{f_2} = \frac{3}{4}\frac{u}{(\varepsilon+1)^2 + (\varepsilon+1)\sqrt{u}} \tag{43}$$

where
$$u = \left(\varepsilon^2+\varepsilon\right)/2 \tag{44}$$

For convenience, the optimum damping ratio is chosen to be the root mean square value $\xi_r^2\Big|_{f_1}$ and $\xi_r^2\Big|_{f_2}$ using Eq. (43) and it can be written as

$$\xi_{r\,opt} = \sqrt{\frac{3\varepsilon}{4\varepsilon+8}} \tag{45}$$

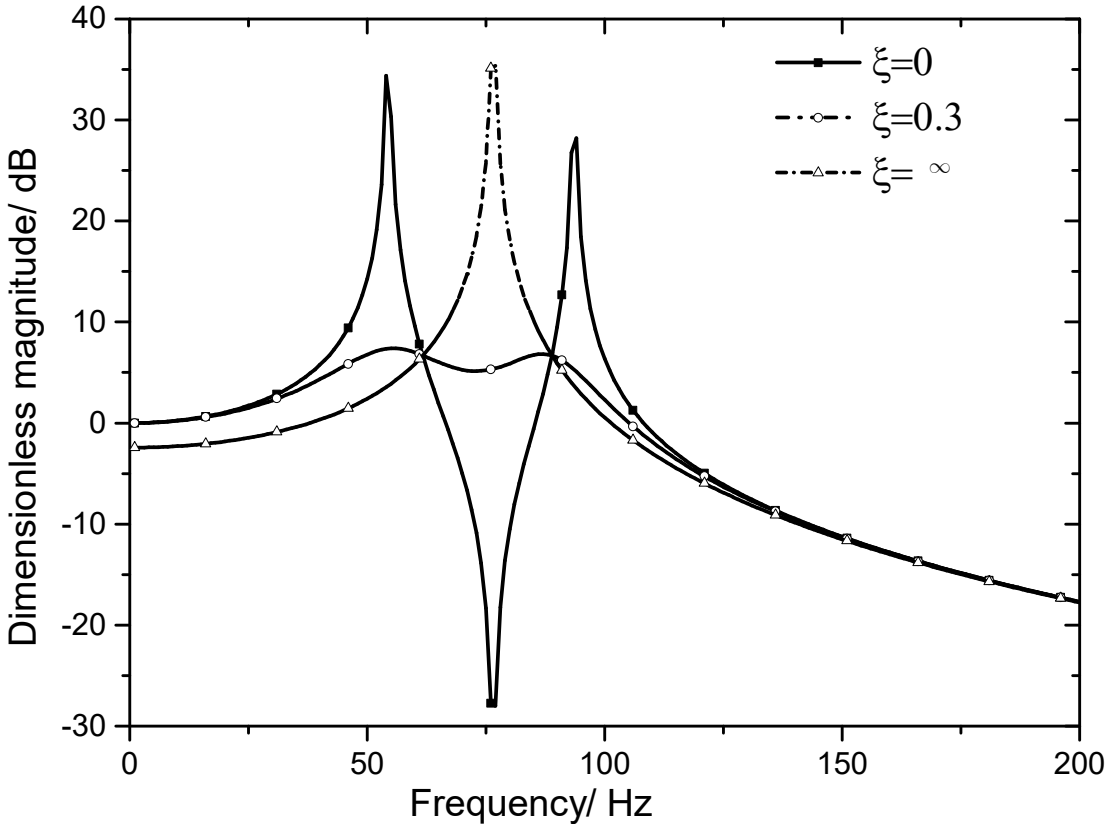

Fig. 6 Dimensionless magnitude of receptance $\left|\tilde{H}(f)\right|$ versus frequency at different damping ratios.

6. Design guideline of the beam absorber

The optimum tuning ratio of the beam absorber in Eq. (41) and the damping ratio in Eq. (45) depend on the term ε as shown in Eq. (38), which is different from the traditional discrete DVAs whose optimum tuning ratio and damping ratio depend solely on the mass ratio [4]. In order to show the relationship of these optimum parameters with the physical parameters (i.e., dimensions and material property of the beam absorber) the dimensionless mode shape functions $\tilde{\phi}_i(\zeta)$ are introduced as

$$\tilde{\phi}_i(\zeta)=\left\{\cos(b_i\zeta)-\cosh(b_i\zeta)+r_i\left[\sin(b_i\zeta)-\sinh(b_i\zeta)\right]\right\},\quad \zeta\in[0,1]$$
$$\text{where}\quad r_i=-\left[\cos(b_i)+\cosh(b_i)\right]/\left[\sin(b_i)+\sinh(b_i)\right]. \tag{46}$$

It should be noted that the dimensionless mode shape function $\tilde{\phi}_i(\zeta)$ in Eq.(46) is different from the mode shape functions $\phi_{1i}(x_1)$ and $\phi_{2i}(x_2)$ defined in Eqs. (13), (14), (26) and (27).

These mode shape functions are normalized to the mass of the beam they belong to and thus they have the unit of $kg^{-1/2}$. On the other hand, Eq. (46) is dimensionless.

$$\mu_N = m_2\phi_{1i}^2(L_1) = \frac{\rho_2 A_2 L_2}{\rho_1 A_1 L_1}\frac{\tilde{\phi}_N^2(1)}{\int_0^1 \tilde{\phi}_N^2(\zeta)d\zeta}$$

$$\text{where} \quad \frac{\tilde{\phi}_N^2(1)}{\int_0^1 \tilde{\phi}_N^2(\zeta)d\zeta} = \begin{cases} 4.001 & N=1 \\ 3.995 & N=2 \\ 4.001 & N=3 \end{cases} \tag{47}$$

$$\lambda_{opt}^2 = \omega_r^2/\bar{\Omega}_N^2 = \omega_r^2(1+\mu_N)/\Omega_N^2 = \frac{b_r^4}{b_N^4}\frac{E_2 I_2/L_2}{E_1 I_1/L_1}\frac{\rho_1 A_1 L_1}{\rho_2 A_2 L_2}\frac{L_1^2}{L_2^2}(1+\mu_N) = 1+\varepsilon \tag{48}$$

$$\varepsilon = \frac{E_2 I_2/L_2}{E_1 I_1/L_1}\frac{\tilde{\phi}_N'^2(1)\tilde{\phi}_r''(0)\int_0^1 \zeta\tilde{\phi}_r(\zeta)d\zeta}{b_N^4\left(\int_0^1 \tilde{\phi}_N^2(\zeta)d\zeta\right)\left(\int_0^1 \tilde{\phi}_r^2(\zeta)d\zeta\right)}$$

$$\text{where} \quad \frac{\tilde{\phi}_r''(0)\int_0^1 \zeta\tilde{\phi}_r(\zeta)d\zeta}{\left(\int_0^1 \tilde{\phi}_r^2(\zeta)d\zeta\right)} = \begin{cases} 3.9999 & r=1 \\ 4.0019 & r=2 \\ 4.0072 & r=3 \end{cases} \quad \text{and} \quad \frac{\tilde{\phi}_N'^2(1)}{b_N^4\left(\int_0^1 \tilde{\phi}_N^2(\zeta)d\zeta\right)} = \begin{cases} 0.6132 & N=1 \\ 0.1883 & N=2 \\ 0.0647 & N=3 \end{cases} \tag{49}$$

The relationship of mass ratio μ_N and ε can be derived by substituting of Eq.(47) and Eq.(49) to Eq. (48).

$$Coeff\left(\frac{L_1^2}{L_2^2}\frac{(1+\mu_N)}{\mu_N}\right) = \frac{1+\varepsilon}{\varepsilon} \tag{50}$$

where

$$Coeff = \frac{\tilde{\phi}_N^2(1)}{\int_0^1 \tilde{\phi}_N^2(\zeta)d\zeta}\left[\frac{\tilde{\phi}_N'^2(1)\tilde{\phi}_r''(0)\int_0^1 \zeta\tilde{\phi}_r(\zeta)d\zeta}{b_N^4\left(\int_0^1 \tilde{\phi}_N^2(\zeta)d\zeta\right)\left(\int_0^1 \tilde{\phi}_r^2(\zeta)d\zeta\right)}\right]^{-1}\frac{b_r^4}{b_N^4}$$

$$= \frac{b_r^4\left(\int_0^1 \tilde{\phi}_r^2(\zeta)d\zeta\right)}{\tilde{\phi}_r''(0)\int_0^1 \zeta\tilde{\phi}_r(\zeta)d\zeta} = \begin{cases} 3.09 & r=1 \\ 121.3 & r=2 \\ 950.04 & r=3 \end{cases}$$

According to Eqs. (47) to (49), once the close resonant frequency orders N and r are determined, μ_N is proportional to the mass ratio of the beam absorber. ε is proportional to the ratio of EI/L. From Eq. (48), the optimum tuning ratio square is dependent on the mass ratio, ratio of EI/L and the length ratio. The relationship of ε and mass ratio is more pronounced in Eq. (50). Under the same mass ratio, Eq. (50) has different sets of solutions of ε and L_1/L_2 that can be achieved by choosing proper material and geometry parameters of the beam DVA. The proper design procedure should be setting ε first according to the

vibration reduction request. Then choose the materials for both beams. After that, put a chosen value of the mass ratio to Eq.(48) and the length ratio is hence derived. The order of obtaining the length ratio and mass ratio can be changed. The three variables, namely the length, width and thickness of the beam absorber, can then be calculated by solving the linear algebraic equations (47), (48) and (49). The detailed derivation of Eqs. (47) to (49) is presented in Appendix C.

7. Comparisons between the beam absorber and the traditional DVA

In this Section, the proposed beam absorber is compared with the traditional single degree-of-freedom spring-mass-damper system. The two types of absorbers are shown in Fig. 7. The same primary cantilever beam is used again here. The geometry of the beam absorber is designed according to the guideline established in Section 6. The dimensionless magnitude of the receptance of the primary beam attached to two types of absorbers are compared.

The receptance of the primary beam attached with a beam absorber as illustrated in Fig. 7a is written as

$$\frac{W(x,s)}{R(s)} = \frac{\phi_{1N}(x)\phi_{1N}(L/2)}{\Omega_N^2} \frac{\left(\lambda^2 - f^2 + i2\xi_r\lambda f\right)}{\left[\left(1-f^2\right)\left(\lambda^2 - f^2\right) - \varepsilon f^2\right] + i2\xi_r\lambda f\left(1+\varepsilon - f^2\right)} = \frac{\phi_{1N}(x)\phi_{1N}(L/2)}{\Omega_N^2}\tilde{H}(f) \tag{51}$$

The dimensionless response magnitude at the two fixed points can be shown to be

$$\left|\tilde{H}(f_1)\right| = \left|\tilde{H}(f_2)\right| = \sqrt{\frac{2}{\varepsilon(\varepsilon+1)}} \tag{52}$$

where ε is the ratio of EI/L between two beams as illustrated in Eq.(49).

The receptance of the primary beam with a traditional DVA attached as illustrated in Fig. 7b is written as

$$\frac{W_t(x,s)}{R(s)} = \frac{\phi_{1N}(x)\phi_{1N}(L/2)}{\Omega_N^2} \frac{\lambda_t^2 - f_t^2 + i2\xi\lambda_t f_t}{\left(\left(1-f_t^2\right)\left(\lambda_t^2 - f_t^2\right) - \mu_N\lambda_t^2 f_t^2\right) + i2\xi\lambda_t f_t\left(1 - f_t^2 - \mu_N f_t^2\right)} = \frac{\phi_{1N}(x)\phi_{1N}(L/2)}{\Omega_N^2}\tilde{H}_t(f_t) \tag{53}$$

where

$$\omega_n = \sqrt{k/m}, \xi = c/(2m\omega_n)$$
$$\lambda_t = \omega_n/\Omega_N, f_t = \omega/\Omega_N, \quad \mu_N = m\phi_{1N}^2(L_1) \tag{54}$$

ω_n and ξ are resonance frequency and damping ratio of the traditional DVA, respectively. μ_N and Ω_N have the same definition as the case of beam absorber. Note λ_t and f_t have different definitions from Eq. (37).

The optimum tuning ratio and damping ratio of the traditional DVA can be derived using the fixed-points theory as a function of μ_N and written as [4]

$$\lambda_{t\ opt} = \frac{1}{1+\mu_N}, \xi_{t\ opt} = \sqrt{\frac{3\mu_N}{8(1+\mu_N)}} \tag{55}$$

The maximum response amplitude may be approximated by the amplitude at the two fixed points written as

$$\left|\tilde{H}_t(f_{t1})\right| = \left|\tilde{H}_t(f_{t2})\right| = \sqrt{\frac{\mu_N+2}{\mu_N}} \tag{56}$$

Using Eqs. (52) and (56), the condition required for the beam absorber to provide larger suppression than the traditional DVA in the targeted mode can be written as

$$\sqrt{\frac{2}{\varepsilon(\varepsilon+1)}} < \sqrt{\frac{\mu_N+2}{\mu_N}} \tag{57}$$

Define the ratio of the maximum amplitude of the two types of DVA as $f(\varepsilon,\mu_N)$ written as

$$f(\varepsilon,\mu_N) = \sqrt{\frac{2\mu_N}{\varepsilon(\varepsilon+1)(\mu_N+2)}} \tag{58}$$

When $f(\varepsilon,\mu_N)<1$, the effect of vibration suppression of the beam absorber outperforms that of the traditional DVA. Eq. (47) shows that μ_N varies from 0.04 to 0.6 when the mass ratio varies from 1% to 15%. The contour plot of $f(\varepsilon,\mu_N)$ is presented in Fig. 8. It is evident that once the mass ratio is fixed, the traditional DVA has fixed optimum value whereas the beam absorber outperforms the traditional DVA by choosing ε above the threshold value as shown by the curve of $f(\varepsilon,\mu_N)=1$ in Fig. 8.

Take the primary beam in Table.1 as an example. The mass ratio is 0.1, then $\mu_N = 0.4$. From Fig. 8, the threshold of ε is close to 0.3. Choose $\varepsilon = 0.3, 0.35, 0.4$. The beam absorber has

the same material properties as in Table. 1. The related dimensions of the beam absorber and the parameters of the traditional DVA are shown in Table.2. The dimensionless magnitude of primary beam attached with the beam absorber and traditional DVA are shown in Fig. 9. The ratios of the maximum amplitude of the two types of DVA $f(\varepsilon, \mu_N)$ are calculated for the three sets of ε = 0.3, 0.35, 0.4 using Eq. (58) to be 0.92, 0.84 and 0.77, respectively. It can be seen that the proposed beam absorber offers further reduction of the resonant vibration of the primary beam by 8%, 16% and 23% respectively, as compared to the traditional DVA. Eq. (50) shows that the higher ε is, the more suppression can be achieved. Reviewing Eq. (48) or Eq. (50), it's fair to say the mass ratio is not a crucial factor in the design of the beam DVA. A better performance of the proposed beam DVA at a fixed mass ratio can be achieved by choosing a higher value of ε and satisfying Eq. (48). Eq. (48) or Eq. (50) reflects the advantage of the proposed DVA. The mass ratio, length ratio and ε of the beam DVA are related. Although the optimum tuning performance and parameters appear to be solely dependent on ε as shown in Eq.(41), they are actually related to the mass ratio and length ratio as well. To some degree, the length ratio, the bending stiffness ratio and the mass ratio involved in Eq.(48) all contribute to the optimum tuning performance by the beam DVA. The presence of the other factors enhances the flexibility of the optimum tuning of the beam DVA. That's why the beam DVA is superior to the traditional DVA under the same mass ratio constraint. Its optimum performance is not solely dependent on the mass ratio as in the case of the traditional DVA.

A further remark is that theoretically there is no limit for the value of ε when the mass ratio is fixed. However, from Eqs. (41) and (45) the higher the value of ε, the higher the damping ratio and tuning ratio will be. So in practice, the choice of ε depends on whether the tuning and the damping ratios can satisfy Eq.(48) and Eq.(45), respectively.

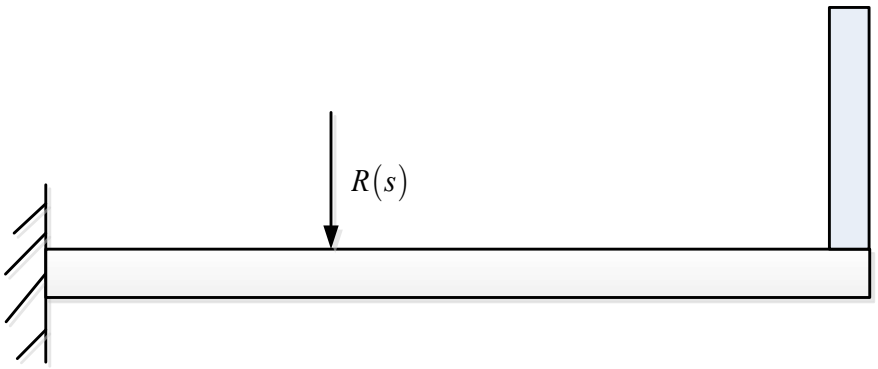

(a)

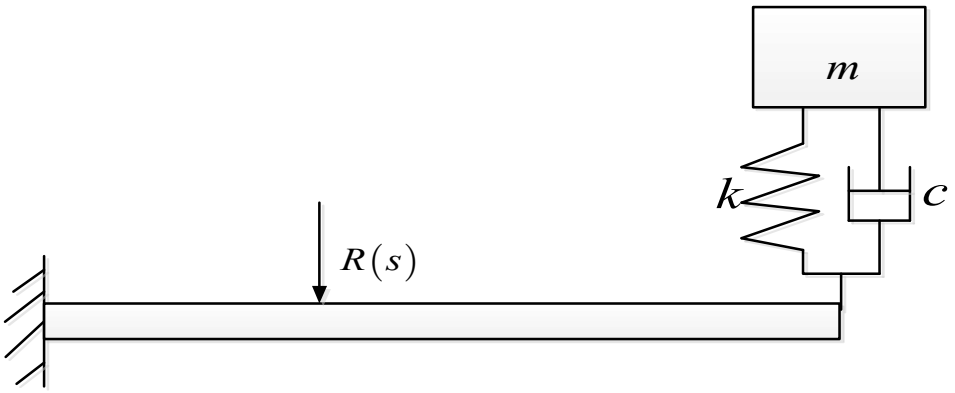

(b)

Fig. 7 (a) The primary beam connected with a beam absorber

(b) The primary beam connected with a traditional DVA

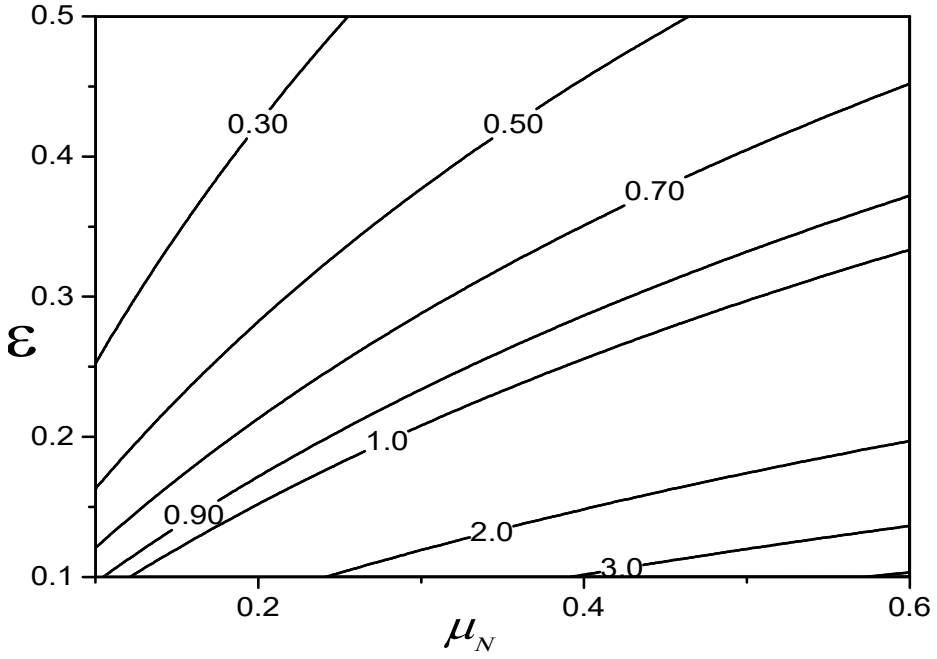

Fig. 8 The contour plot of $f(\varepsilon, \mu_N)$

Table 2 The optimum parameters of the beam absorber and the traditional DVA

$\mu_N = 0.4$	Beam Absorber					Traditional DVA
	Length / mm	Width / mm	Thickness / mm	modal damping ratio ξ_{opt} Eq.(45)	$f(\varepsilon, \mu_N)$ Eq.(58)	$m = 0.0207$ Kg, $k = 2519.4$ N/m, $c = 4.725$ N/(ms^{-1})
$\varepsilon = 0.3$	170.4	16.2	2.7	0.31	*0.92*	
$\varepsilon = 0.35$	180.6	13.4	3.1	0.33	*0.84*	
$\varepsilon = 0.4$	189.6	11.4	3.5	0.35	*0.77*	

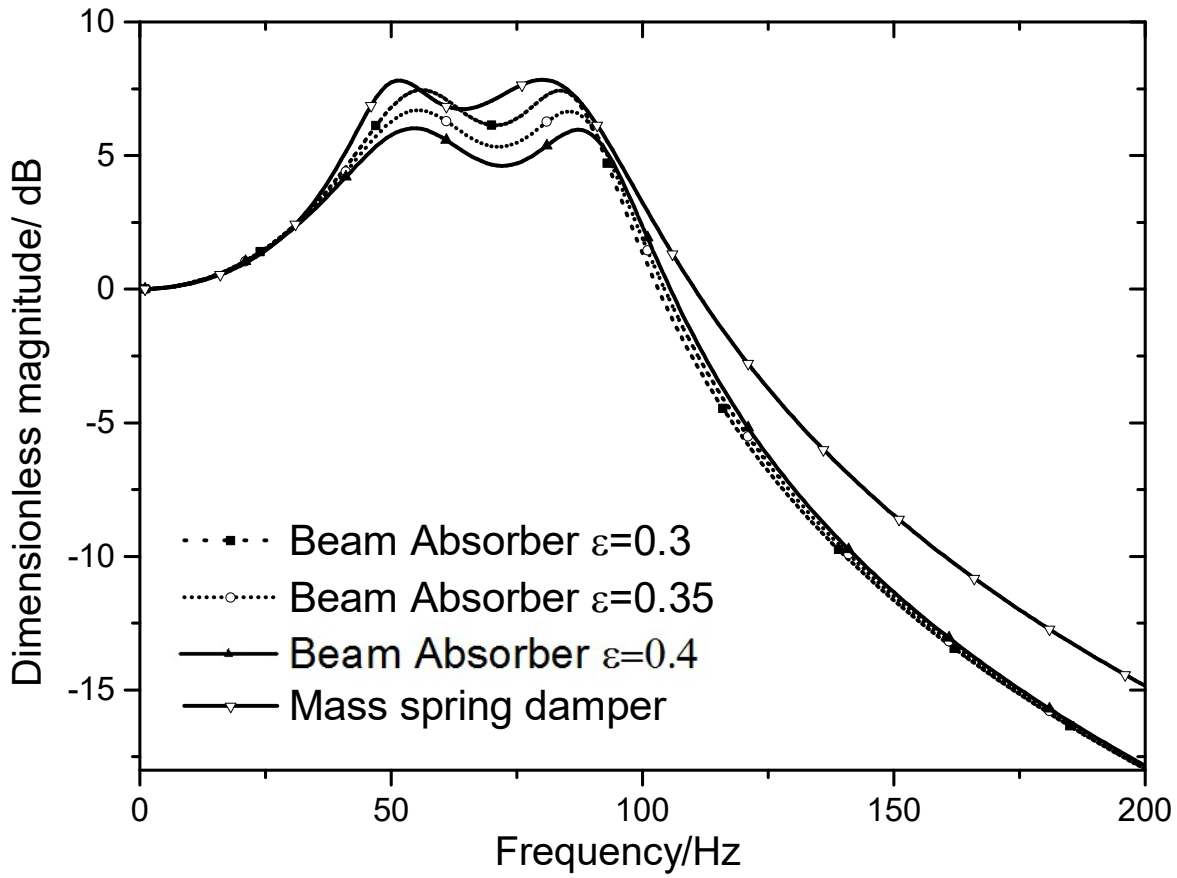

Fig. 9 Dimensionless magnitudes of the receptance of the traditional DVA $\left|\tilde{H}_t(f)\right|$ and that of the beam absorber $\left|\tilde{H}(f)\right|$ with ε = 0.3, 0.35,0.4 and μ_N = 0.4.

8. Conclusions

A beam-based DVA is proposed and compared to the traditional discrete type of DVA (i.e, the mass-spring-damper system). The proposed beam absorber can achieve more vibration reduction under the same mass ratio than the traditional DVA due to the flexibility in the design of its geometry and physical properties. It can also address the vibration resonances at low frequency more conveniently by changing its geometry shape to attain the target low frequency. By combining the receptance theory with the fixed-points theory, analytical expressions of the optimum tuning ratio and damping ratio of the continuous beam-based DVA are derived to guide the absorber design. The traditional mass spring damper's optimal performance is constrained by the mass ratio. However, this study shows that there exists a set of optimal material and geometry parameters which allows the beam absorber to outperform its mass-spring-damper counterpart under the same mass ratio constraints. A design guideline is established to choose the material and geometry parameters of the beam absorber. The proposed absorber may be applied to suppress resonant vibrations of flexible robotic arms in the future.

Acknowledgment

The author wishes to acknowledge the research funding support from University Grant Council of Hong Kong SAR (Project: B-Q47U) and The Hong Kong Polytechnic University of Hong Kong.

References

[1] C.L. Lee, Y.T. Chen, L.L. Chung, Y.P. Wang, Optimal design theories and applications of tuned mass dampers, Engineering structures, 28 (2006) 43-53.

[2] J.R. Sladek, R.E. Klingner, Effect of tuned-mass dampers on seismic response, Journal of structural engineering, 109 (1983) 2004-2009.

[3] K. Tse, K. Kwok, Y. Tamura, Performance and cost evaluation of a smart tuned mass damper for suppressing wind-induced lateral-torsional motion of tall structures, Journal of Structural Engineering, 138 (2012) 514-525.

[4] J.P. Den Hartog, Mechanical vibrations, Courier Corporation, 1985.

[5] G. Warburton, Optimum absorber parameters for minimizing vibration response, Earthquake engineering and structural dynamics, 9 (1981) 251-262.

[6] G. Warburton, Optimum absorber parameters for various combinations of response and excitation parameters, Earthquake Engineering & Structural Dynamics, 10 (1982) 381-401.

[7] T. Asami, O. Nishihara, A.M. Baz, Analytical Solutions to H infinity and H2 Optimization of Dynamic Vibration Absorbers Attached to Damped Linear Systems, Journal of vibration and acoustics 124 (2002), 284-295.

[8] Y.L. Cheung, W.O. Wong, H∞ and H2 optimizations of a dynamic vibration absorber for suppressing vibrations in plates, Journal of Sound and Vibration, 320 (2009) 29-42.

[9] J. Dayou, Fixed-points theory for global vibration control using vibration neutralizer, Journal of Sound and Vibration, 292 (2006) 765-776.

[10] Y.L. Cheung, W.O. Wong, H-infinity optimization of a variant design of the dynamic vibration absorber—Revisited and new results, Journal of sound and vibration, 330 (2011) 3901-3912.

[11] Y.L. Cheung, W.O. Wong, L. Cheng, Optimization of a hybrid vibration absorber for vibration control of structures under random force excitation, Journal of Sound and Vibration, 332 (2013) 494-509.

[12] Y.L. Cheung, W.O. Wong, L. Cheng, Minimization of the mean square velocity response of dynamic structures using an active-passive dynamic vibration absorber, The Journal of the Acoustical Society of America, 132 (2012) 197-207.

[13] Y.L. Cheung, W.O. Wong, L. Cheng, Design optimization of a damped hybrid vibration absorber, Journal of sound and vibration, 331 (2012) 750-766.

[14] M.H. Tso, J. Yuan, W.O. Wong, Suppression of random vibration in flexible structures using a hybrid vibration absorber, Journal of sound and vibration, 331 (2012) 974-986.

[15] E. Rustighi, M. Brennan, B. Mace, A shape memory alloy adaptive tuned vibration absorber: design and implementation, Smart Materials and Structures, 14 (2004) 19.

[16] M.A. Acar, C. Yilmaz, Design of an adaptive–passive dynamic vibration absorber composed of a string–mass system equipped with negative stiffness tension adjusting mechanism, Journal of sound and vibration, 332 (2013) 231-245.

[17] C.L. Lee, Y.T. Chen, L.L. Chung, Y.P. Wang, Optimal design theories and applications of tuned mass dampers, Engineering structures, 28 (2006) 43-53.

[18] Chunxiang. Li, Performance of multiple tuned mass dampers for attenuating undesirable oscillations of structures under the ground acceleration, Earthquake Engineering & Structural Dynamics, 29 (2000) 1405-1421.

[19] T. Aida, S. Toda, N. Ogawa, Y. Imada, Vibration Control of Beams by Beam-Type Dynamic Vibration Absorbers, Journal of Engineering Mechanics, 118 (1992) 248-258.

[20] D.J. Mead, Passive vibration control, John Wiley & Sons Inc, 1999.

[21] H.T. Banks, D.J. Inman, On damping mechanisms in beams. ASME Journal of Applied Mechanics, 58 (1991) 716–23

[22] H.A. Sodano, A. Erturk, J.M. Renno, D.J. Inman, Modeling of piezoelectric energy harvesting from an L-shaped beam-mass structure with an application to UAVs, Journal of intelligent material systems and structures, 20 (2009) 529-544.

Appendix A

This appendix develops the analytical model of cantilever beam with support rotation.

The cantilever beam suffers from the support rotation is shown in Fig. A.1 and is modeled as an Euler-Bernoulli beam. E is the elastic modulus, I is the moment of the beam, m is the mass of per unit length, A is the cross-Section area and l is the length of the beam. The total displacement of one point on the cantilever beam under the base excitation is defined as:

$$w(x,t) = \theta(t)x + \varphi(x,t) \tag{A.1}$$

where $\varphi(x,t)$ is the deflection curve, $\theta(t)$ is the rotation angle from the ground.

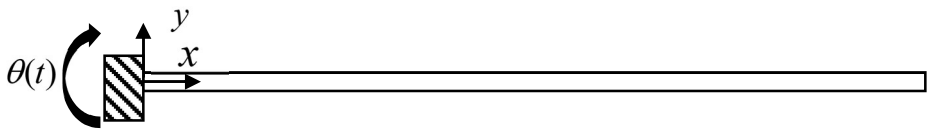

Fig.A.1. Cantilever beam under base rotation

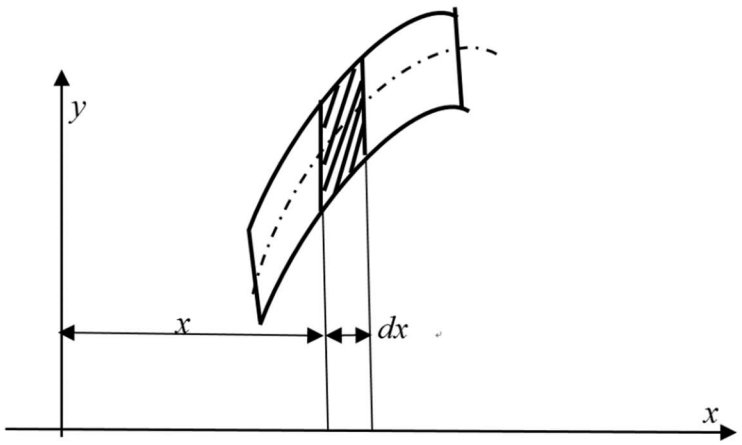

Fig.A.2. A small segment of beam

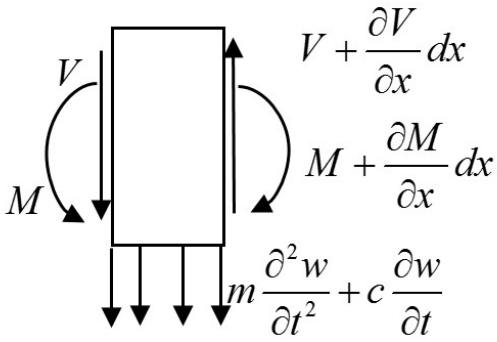

Fig.A.3. Force analysis on the cross Section

As illustrated in Ref. [21], one types of damping force are taken into consideration: external damping force which is proportional to velocity and represented as $-c\frac{\partial w}{\partial t}$. From material mechanics, the bending strain and the deflection of the beam is:

$$\varepsilon_b = -y\frac{\partial^2 \varphi(x,t)}{\partial x^2} \tag{A.2}$$

Then the total bending moment of the small segment is:

$$M = -EI\frac{\partial^2 w(x,t)}{\partial x^2} = -EI\frac{\partial^2 \varphi(x,t)}{\partial x^2} \tag{A.3}$$

The shear force and the moment has the following relationship:

$$V = \frac{\partial M}{\partial x} = \frac{\partial\left(-EI\dfrac{\partial^2 \varphi(x,t)}{\partial x^2}\right)}{\partial x} \tag{A.4}$$

According to the force balance of the whole small segment, the dynamics equation of the small segment can be derived:

$$V+\frac{\partial V}{\partial x}dx - V - \left[m\frac{\partial^2 w(x,t)}{\partial t^2}+c\frac{\partial w(x,t)}{\partial t}\right]dx = 0 \tag{A.5}$$

Substituting the expression of $w(x,t)$ in (A.1) into (A.5), the Eq. (A.5) becomes:

$$\frac{\partial V}{\partial x}dx - \left[m\frac{\partial^2 \varphi(x,t)}{\partial t^2}+c\frac{\partial \varphi(x,t)}{\partial t}+m\frac{\partial^2 \theta(t)}{\partial t^2}x+c\frac{\partial \theta(t)}{\partial t}x\right]dx = 0 \tag{A.6}$$

Substituting the expression of V in (A.4) to (A.6) can yield the movement equation of the small segment under the base rotational excitation and it is shown as:

$$EI\frac{\partial^4 \varphi(x,t)}{\partial x^4}+c\frac{\partial \varphi(x,t)}{\partial t}+\rho A\frac{\partial^2 \varphi(x,t)}{\partial t^2} = -c\dot{\theta}(t)x-\rho A\ddot{\theta}(t)x \tag{A.7}$$

Appendix B

This appendix presents the derivation of transfer matrix of Bernoulli-Euler Beam.

The dynamic equation of motion of the beam may be written as

$$EI\frac{\partial^4 w}{\partial x^4}+\rho A\frac{\partial^2 w}{\partial t^2}=0 \tag{B.1}$$

Assume that the solution of harmonic oscillation can be written as

$$w(x,t)=W(x)\mathrm{e}^{i\omega t} \tag{B.2}$$

The non-dimensional characteristic equation of the equation is

$$\begin{aligned}&\left(EID^4/L^4-\rho A\omega^2\right)W(\xi)=0,\\&D=d/d\xi,\xi=x/L\end{aligned} \tag{B.3}$$

Assume that the solution of $W(\xi)$ can be written as

$$W(\xi)=\sum_{i=1}^{4}R_i e^{r_i\xi},\Theta(\xi)=\frac{\partial W}{L\partial\xi}=\sum_{i=1}^{4}R_i\frac{r_i}{L}e^{r_i\xi},S(\xi)=EI\frac{\partial^3 W}{L^3\partial\xi^3},\mathrm{M}(\xi)=-EI\frac{\partial^2 W}{L^2\partial\xi^2} \tag{B.4}$$

where r_i is the root of the characteristic equation Eq. (B.5).

$$EIr_i^4/L^4-\rho A\omega^2=0 \tag{B.5}$$

$$\begin{aligned}&\delta=\{W(0)\quad\Theta(0)\quad W(1)\quad\Theta(1)\},\delta=BR\\&F=\{S(0)\quad M(0)\quad S(1)\quad M(1)\},F=AR\end{aligned} \tag{B.6}$$

$$F=AB^{-1}\delta=K\delta \tag{B.7}$$

$$\begin{Bmatrix}W(1)\\\Theta(1)\\S(1)\\M(1)\end{Bmatrix}=T\begin{Bmatrix}W(0)\\\Theta(0)\\S(0)\\M(0)\end{Bmatrix} \tag{B.8}$$

$$\begin{aligned}&T_{11}=-K_{12}^{-1}K_{11},T_{12}=K_{12}^{-1}\\&T_{21}=-K_{21}+K_{22}K_{12}^{-1}K_{11},T_{22}=-K_{22}K_{12}^{-1}\end{aligned} \tag{B.9}$$

Similarly, the transfer matrix of axial vibration rod can be obtained.

The dynamic equation of the axial vibration rod is

$$\rho \frac{\partial^2 u}{\partial t^2} - E \frac{\partial^2 u}{\partial t^2} = 0 \tag{B.10}$$

The axial force in the rod is

$$F = EA \frac{\partial u}{\partial x} \tag{B.11}$$

The same way as we derive the transfer matrix of the transverse vibration of the beam, we can obtain the transfer matrix of the axial vibration written as

$$\begin{Bmatrix} U(1) \\ F(1) \end{Bmatrix} = T \begin{Bmatrix} U(0) \\ F(0) \end{Bmatrix} \tag{B.12}$$

So we can get the transfer matrix of an Euler-Bernoulli beam by taking axial deformation into consideration.

$$\begin{Bmatrix} U(L) \\ W(L) \\ \Theta(L) \\ F(L) \\ S(L) \\ M(L) \end{Bmatrix} = T \begin{Bmatrix} U(0) \\ W(0) \\ \Theta(0) \\ F(0) \\ S(0) \\ M(0) \end{Bmatrix} \tag{B.13}$$

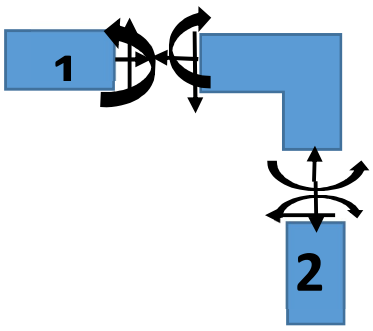

Fig.B.1 the displacement and force relationship of the two beams at the connecting point

In the 90 degree rotational angle，the displacement and force of the two beam satisfies the following:

$$\begin{Bmatrix} U_2 \\ W_2 \\ \Theta_2 \\ F_2 \\ S_2 \\ M_2 \end{Bmatrix} = \begin{bmatrix} 0 & 1 & 0 & 0 & 0 & 0 \\ -1 & 0 & 0 & 0 & 0 & 0 \\ 0 & 0 & 1 & 0 & 0 & 0 \\ 0 & 0 & 0 & 0 & 1 & 0 \\ 0 & 0 & 0 & -1 & 0 & 0 \\ 0 & 0 & 0 & 0 & 0 & 1 \end{bmatrix} \begin{Bmatrix} U_1 \\ W_1 \\ \Theta_1 \\ F_1 \\ S_1 \\ M_1 \end{Bmatrix} \tag{B.14}$$

So the whole transfer matrix in the L-shaped beam can be written as:

$$\begin{Bmatrix} U \\ W \\ \Theta \\ F \\ S \\ M \end{Bmatrix}_{free} = T_{abeam} T_{rot} T_{pbeam} \begin{Bmatrix} U \\ W \\ \Theta \\ F \\ S \\ M \end{Bmatrix}_{fixed} \tag{B.15}$$

So we can get the displacement response at any point of the beam using Eq. (B.15).

Appendix C

This appendix presents the detailed derivation of Eqs. (47) to (49).

$$\begin{aligned}&\phi_{1i}(x_1)=A_{1i}\left\{\cos(b_i x_1/L_1)-\cosh(b_i x_1/L_1)+r_{1i}\left[\sin(b_i x_1/L_1)-\sinh(b_i x_1/L_1)\right]\right\}\\&r_{1i}=-\left[\cos(b_i)+\cosh(b_i)\right]/\left[\sin(b_i)+\sinh(b_i)\right]\end{aligned} \tag{C.1}$$

$$\int_0^{L_1}\rho_1 A_1\phi_{1i}(x_1)\phi_{1j}(x_1)dx_1=\delta_{ij} \tag{C.2}$$

b_i correspond to 1.875, 4.694 and 7.855 for the first three modes.

$$\begin{aligned}&\phi_{2i}(x_2)=A_{2i}\left\{\cos(b_i x_2/L_2)-\cosh(b_i x_2/L_2)+r_{2i}\left[\sin(b_i x_2/L_2)-\sinh(b_i x_2/L_2)\right]\right\}\\&r_{2i}=-\left[\cos(b_i)+\cosh(b_i)\right]/\left[\sin(b_i)+\sinh(b_i)\right]\end{aligned} \tag{C.3}$$

$$\int_0^{L_2}\rho_2 A_2\phi_{2i}(x_2)\phi_{2j}(x_2)dx_2=\delta_{ij} \tag{C.4}$$

Assume that the mode shape function without coefficient can be written in the following form:

$$\begin{aligned}&\tilde{\phi}_i(\zeta)=\left\{\cos(b_i\zeta)-\cosh(b_i\zeta)+r_i\left[\sin(b_i\zeta)-\sinh(b_i\zeta)\right]\right\}\\&r_i=-\left[\cos(b_i)+\cosh(b_i)\right]/\left[\sin(b_i)+\sinh(b_i)\right]\\&\zeta\in[0,1]\end{aligned} \tag{C.5}$$

Eq. (C.2) and Eq. (C.4) can be rewritten into the following form:

$$\rho_1 A_1 L_1 A_{1i}^2\int_0^1\tilde{\phi}_i(\zeta)\tilde{\phi}_j(\zeta)d\zeta=\delta_{ij} \tag{C.6}$$

$$\rho_2 A_2 L_2 A_{2i}^2\int_0^1\tilde{\phi}_i(\zeta)\tilde{\phi}_j(\zeta)d\zeta=\delta_{ij} \tag{C.7}$$

$$A_{1i}=1\Big/\sqrt{\left(\rho_1 A_1 L_1\int_0^1\tilde{\phi}_i^2(\zeta)d\zeta\right)} \tag{C.8}$$

$$A_{2i}=1\Big/\sqrt{\left(\rho_2 A_2 L_2\int_0^1\tilde{\phi}_i^2(\zeta)d\zeta\right)} \tag{C.9}$$

From Eq. (17), we can derive μ_N based on $\tilde{\phi}_N$:

$$\begin{aligned}\mu_N&=\rho_2 A_2 L_2\phi_{1N}^2(L_1)=\rho_2 A_2 L_2 A_{1N}^2\tilde{\phi}_N^2(1)\\&=\frac{\rho_2 A_2 L_2}{\rho_1 A_1 L_1}\frac{\tilde{\phi}_N^2(1)}{\int_0^1\tilde{\phi}_N^2(\zeta)d\zeta}\end{aligned} \tag{C.10}$$

From Eq. (31), g_i can be written based on $\tilde{\phi}_i$:

$$g_i = -\rho_2 A_2 \int_0^{L_2} x_2 \phi_{2i}(x_2) dx_2 = -\rho_2 A_2 L_2^2 \int_0^1 \zeta \tilde{\phi}_i(\zeta) d\zeta \Big/ \sqrt{\left(\rho_2 A_2 L_2 \int_0^1 \tilde{\phi}_i^2(\zeta) d\zeta\right)} \tag{C.11}$$

$$\phi'_{1k}(x) = \tilde{\phi}'_k\left(x/L_1\right) \Big/ L_1 \sqrt{\left(\rho_1 A_1 L_1 \int_0^1 \tilde{\phi}_k^2(\zeta) d\zeta\right)} \tag{C.12}$$

$$\phi''_{2r}(x) = \tilde{\phi}''_r\left(x/L_2\right) \Big/ L_2^2 \sqrt{\left(\rho_2 A_2 L_2 \int_0^1 \tilde{\phi}_r^2(\zeta) d\zeta\right)} \tag{C.13}$$

The N^{th} order natural frequency of the primary beam and the r^{th} order natural frequency of the beam absorber can be written as:

$$\begin{aligned} \Omega_N^2 &= b_N^4 E_1 I_1 \Big/ \left(\rho_1 A_1 L_1^4\right) \\ \omega_r^2 &= b_r^4 E_2 I_2 \Big/ \left(\rho_2 A_2 L_2^4\right) \end{aligned} \tag{C.14}$$

From Eq. (38), ε is obtained based on $\tilde{\phi}_k, \tilde{\phi}_r$:

$$\begin{aligned} \varepsilon &= E_2 I_2 \phi'^2_{1N}(L_1) g_r \phi''_{2r}(0) \Big/ \left[\Omega_N^2\right] \\ &= \frac{E_2 I_2 \tilde{\phi}'^2_N(1) \tilde{\phi}''_r(0) \rho_2 A_2 L_2^2 \int_0^1 \zeta \tilde{\phi}_r(\zeta) d\zeta \left(\rho_1 A_1 L_1^4\right)}{L_1^2 \left(\rho_1 A_1 L_1 \int_0^1 \tilde{\phi}_N^2(\zeta) d\zeta\right) L_2^2 \left(\rho_2 A_2 L_2 \int_0^1 \tilde{\phi}_r^2(\zeta) d\zeta\right) b_N^4 E_1 I_1} \\ &= \frac{E_2 I_2 / L_2}{E_1 I_1 / L_1} \frac{\tilde{\phi}'^2_N(1) \tilde{\phi}''_r(0) \int_0^1 \zeta \tilde{\phi}_r(\zeta) d\zeta}{b_N^4 \left(\int_0^1 \tilde{\phi}_N^2(\zeta) d\zeta\right)\left(\int_0^1 \tilde{\phi}_r^2(\zeta) d\zeta\right)} \end{aligned} \tag{C.15}$$

From Eq. (48), we can derive the tuning ratio:

$$\begin{aligned} \lambda_{opt}^2 &= \omega_r^2 / \bar{\Omega}_N^2 = \omega_r^2 \left(1 + \mu_N\right) / \Omega_N^2 \\ &= \frac{b_r^4}{b_N^4} \frac{E_2 I_2 / L_2}{E_1 I_1 / L_1} \frac{\rho_1 A_1 L_1}{\rho_2 A_2 L_2} \frac{L_1^2}{L_2^2} \left(1 + \mu_N\right) = 1 + \varepsilon \end{aligned} \tag{C.16}$$